



# Oligomerization and Spatial Distribution of Kv $\beta$ 1.1 and Kv $\beta$ 2.1 Regulatory Subunits

Sara R. Roig<sup>1,2</sup>, Silvia Cassinelli<sup>1</sup>, Andre Zeug<sup>3</sup>, Evgeni Ponimaskin<sup>3</sup> and Antonio Felipe<sup>1\*</sup>

<sup>1</sup>Molecular Physiology Laboratory, Departament de Bioquímica i Biomedicina Molecular, Institut de Biomedicina (IBUB), Universitat de Barcelona, Barcelona, Spain, <sup>2</sup>Imaging Core Facility, Biozentrum, University of Basel, Basel, Switzerland, <sup>3</sup>Department of Cellular Neurophysiology, Hannover Medical School, Hannover, Germany

Members of the regulatory Kv $\beta$  family modulate the kinetics and traffic of voltage-dependent K<sup>+</sup> (Kv) channels. The crystal structure of Kv channels associated with Kv $\beta$  peptides suggests a  $\alpha$ 4/ $\beta$ 4 composition. Although Kv $\beta$ 2 and Kv $\beta$ 1 form heteromers, evidence supports that only Kv $\beta$ 2.1 forms tetramers in the absence of  $\alpha$  subunits. Therefore, the stoichiometry of the Kv $\beta$  oligomers fine-tunes the activity of hetero-oligomeric Kv channel complexes. We demonstrate that Kv $\beta$  subtypes form homo- and heterotetramers with similar affinities. The Kv $\beta$ 1.1/Kv $\beta$ 2.1 heteromer showed an altered spatial distribution in lipid rafts, recapitulating the Kv $\beta$ 1.1 pattern. Because Kv $\beta$ 2 is an active partner of the Kv1.3-TCR complex at the immunological synapse (IS), an association with Kv $\beta$ 1 would alter this location, shaping the immune response. Differential regulation of Kv $\beta$ s influences the traffic and architecture of the Kv $\beta$  heterotetramer, modulating Kv $\beta$ -dependent physiological responses.

**Keywords:** regulatory subunits, oligomerization, potassium channels, lipid rafts, leukocytes

## INTRODUCTION

The association of  $\alpha$ -conducting subunits with  $\beta$  regulatory peptides determines the functional diversity of voltage-gated potassium (Kv) currents. Thus, changes in the expression of a subunit shape the channel composition and the physiological properties of the channelosome (Pongs and Schwarz, 2010).

Three genes (Kv $\beta$ 1-3) encode the Kv $\beta$  family, some undergoing alternative splicing (i.e., Kv $\beta$ 1.1–Kv $\beta$ 1.3). Kv $\beta$ s exhibit 85% similarity, mostly at the C-terminus. However, several functional differences, focused on Kv modulation, have been described (Kilfoil et al., 2013). While Kv $\beta$ 1 and Kv $\beta$ 3 accelerate the fast inactivation of Kv channels, using a ball-and-chain mechanism (Heinemann et al., 1995; Leicher et al., 1996), Kv $\beta$ 2 increases the surface expression of the complex (Shi et al., 1996). Kv $\beta$  peptides exhibit aldo-keto reductase (AKR) activity by binding to NADP(H) and are included in the AKR6A subfamily within the AKR superfamily (Hyndman et al., 2003). Biochemical and structural evidence confirmed the presence of more than one Kv $\beta$  subunit in a tetrameric Kv channel configuration (Parcej et al., 1992; Gulbis et al., 1999). Scarce information is available regarding the oligomeric formation of Kv $\beta$  peptides. Evidence suggests that Kv $\beta$ 1 and Kv $\beta$ 2 form homo and hetero-oligomeric compositions (Xu et al., 1998; Nystoriak et al., 2017). Atomic force and electron microscopy support that the complex architecture is a tetramer with possible intermediate structures (van Huizen et al., 1999). The Kv $\beta$ 2 crystal determines not only the macromolecular structure but also the orientation of units (Gulbis et al., 1999).

## OPEN ACCESS

### Edited by:

John Bankston,  
University of Colorado Anschutz  
Medical Campus, United States

### Reviewed by:

Gucan Dai,  
Saint Louis University, United States  
Fan Yang,  
Zhejiang University, China

### \*Correspondence:

Antonio Felipe  
afelipe@ub.edu

### Specialty section:

This article was submitted to  
Membrane Physiology and Membrane  
Biophysics,  
a section of the journal  
Frontiers in Physiology

**Received:** 28 April 2022

**Accepted:** 02 June 2022

**Published:** 17 June 2022

### Citation:

Roig SR, Cassinelli S, Zeug A,  
Ponimaskin E and Felipe A (2022)  
Oligomerization and Spatial  
Distribution of Kv $\beta$ 1.1 and Kv $\beta$ 2.1  
Regulatory Subunits.  
Front. Physiol. 13:930769.  
doi: 10.3389/fphys.2022.930769

The molecular determinants for Kv $\beta$  oligomeric formation are mainly located within the core region. Kv $\beta$ 1.1 and Kv $\beta$ 2.1 share most of the C-terminal sequence, but Kv $\beta$ 1.1 presents no interacting domains. Regarding the function of Kv, evidence shows that the higher the expression of Kv $\beta$ 1 is, the larger the inactivation rate. Therefore, the variable stoichiometry of  $\alpha_4\beta_n$  (4  $\alpha$ -subunits with a flexible number of  $\beta$ -subunits) would exert important physiological consequences (Xu et al., 1998). Thus, Kv $\beta$ 2 inhibits the Kv $\beta$ 1-mediated inactivation of Kv channels. This effect requires the core part of the subunit, which is necessary not only for homo- and hetero-oligomerization but also for interaction with the channel. Kv $\beta$ 2 interacts with Kv channels in a tetrameric structure displacing Kv $\beta$ 1, leading to a nonconcentration dependence of Kv modulation (Xu and Li, 1997). However, similar to Kv $\beta$ 2, the capacity of Kv $\beta$ 1.2 to form homo-oligomers has also been documented. Therefore, hybrids of both proteins with Kv channels induce intermediate inactivation patterns on Kv1.2 (Accili et al., 1997). This function could be of special relevance in immune system physiology, where Kv $\beta$  peptides are tightly regulated under insults (McCormack et al., 1999; Vicente et al., 2005). Kv $\beta$ 2 concentrates with Kv1.3 at the immunological synapse (IS) (Beeton et al., 2006; Roig et al., 2022). Furthermore, Kv $\beta$ 2, located in lipid rafts, may cluster in these spots, independent of the channel, during the immune response (Roig et al., 2022). Unlike Kv $\beta$ 1, this spatial regulation is dependent on palmitoylation. The fact that Kv $\beta$ 1.1 may alter the Kv $\beta$ 2 spatial location at the IS, influencing the Kv1.3-dependent physiological consequences, could be crucial during the immune response.

Evidence suggest that Kv $\beta$  peptides could have physiological functions, such as REDOX sensors and clustering targeting proteins to specific spots, without the participation of Kv  $\alpha$  subunits (Beeton et al., 2006; Roig et al., 2022). In this context, our results demonstrated that Kv $\beta$ 1.1, as well as Kv $\beta$ 2.1, are tetramers. In addition, we found that the affinity to form Kv $\beta$  homo- and hetero-oligomers is similar. Both Kv $\beta$  subunits reach the cell surface in homo- and heteromeric forms but with different plasma membrane distributions. While Kv $\beta$ 2.1 partially targets lipid rafts, the combination with Kv $\beta$ 1.1 mistargeted these domains. Therefore, Kv $\beta$ 1, whose abundance is under tight regulation, would fine-tune the final fate and stoichiometry of the functional Kv $\beta$  complex, thereby shaping Kv1.3-dependent physiological responses.

## MATERIALS AND METHODS

### Expression Plasmids, Cell Culture and Transfections

mKv $\beta$ 1.1 and mKv $\beta$ 2.1 were provided by M.M. Tamkun (Colorado State University). mKv $\beta$ 1.1 and mKv $\beta$ 2.1 were subcloned into pEYFP-N1 and pECFP-N1 (Clontech). All constructs were verified by sequencing.

HEK-293 cells were cultured in DMEM (Lonza) containing 10% fetal bovine serum (FBS) supplemented with penicillin (10,000 U/ml), streptomycin (100  $\mu$ g/ml) and L-glutamine

(4 mM) (Gibco). Human Jurkat T-lymphocytes and the murine CY15 dendritic cell line were cultured in RPMI culture medium (Lonza) containing 10% heat-inactivated FBS and supplemented with 10,000 U/ml penicillin, 100  $\mu$ g/ml streptomycin and 2 mM L-glutamine (Gibco). Human CD4<sup>+</sup> T-cell subsets were isolated from peripheral whole blood using a negative selection Rosette Sep<sup>TM</sup> kit from STEMCELL<sup>TM</sup> Technologies. Human T lymphocytes were cultured as previously described (Capera et al., 2021). Murine bone marrow-derived macrophages (BMDMs) from 6- to 10-week-old BALB/c mice (Charles River Laboratories) were used. The cells were isolated and cultured as described elsewhere (Sole et al., 2013).

For confocal imaging and coimmunoprecipitation experiments, cells were seeded (70–80% confluence) in 6-well dishes containing polylysine-coated coverslips or 100 mm dishes 24 h before transfection with selected cDNAs. Lipotransfectina<sup>®</sup> (Attendbio Research) was used for transfection according to the supplier's instructions. The amount of transfected DNA was 4  $\mu$ g for a 100 mm dish and 500 ng for each well of a 6-well dish (for coverslip use). Next, 4–6 h after transfection, the mixture was removed from the dishes and replaced with fresh culture medium. All experiments were performed 24 h after transfection.

### Protein Extraction, Coimmunoprecipitation and Western Blotting

All experimental protocols were approved by the ethical committee of the Universitat de Barcelona in accordance with the European Community Council Directive 86/609 EEC. We also confirm that all experiments were carried out in compliance with the ARRIVE guidelines (<https://arriveguidelines.org>). Rats and mice were briefly anesthetized with isoflurane, and brains and femurs were extracted immediately after euthanasia. The brain was homogenized in RIPA lysis buffer (1% Triton X-100, 1% sodium deoxycholate, 0.1% SDS, 50 mM Tris-HCl pH 8.0, 150 mM NaCl) supplemented with protease inhibitors. Total lysates were spun for 10 min at  $\times$ 10,000 g to remove debris. Supernatants were used to analyze protein expression by western blotting.

Cells were washed twice in cold PBS and lysed on ice with lysis buffer (5 mM HEPES, 150 mM NaCl, 1% Triton X100, pH 7.5) supplemented with 1  $\mu$ g/ml aprotinin, 1  $\mu$ g/ml leupeptin, 1  $\mu$ g/ml pepstatin and 1 mM phenylmethylsulfonyl fluoride as protease inhibitors. Cells were scraped and transferred to a 1.5 ml tube. Then, they were incubated for 20 min at the orbital at 4°C and spun for 20 min at 14,000 rpm. The supernatant was transferred to a new tube, and the protein contents were determined by using the Bio-Rad Protein Assay (Bio-Rad).

For coimmunoprecipitation, 1 mg of protein from each condition was separated and brought up to a volume of 500  $\mu$ L with lysis buffer for IPs (150 mM NaCl, 50 mM HEPES, 1% Triton X-100, pH 7.4) supplemented with protease inhibitors. Precleaning was performed with 40  $\mu$ L of protein A Sepharose beads (GE Healthcare) in an orbital shaker for 1 h at 4°C. Next, each sample was incubated in a small chromatography column (Bio-Rad Microspin

Chromatography Columns), which contained 2.5  $\mu$ g of anti-GFP antibody (Genescript) previously crosslinked to protein A Sepharose beads, for 2 h at room temperature (RT) with continuous mixing. Next, columns were centrifuged for 30 s at  $\times 1,000$  g. The supernatant (SN) was kept and stored at  $-20^{\circ}\text{C}$ . The columns were washed four times with 500  $\mu$ L of lysis buffer and centrifuged for 30 s at  $\times 1,000$  g. Finally, elution was performed by incubating the columns with 100  $\mu$ L of 0.2 M glycine pH 2.5 and spun 30 s at  $\times 1,000$  g. The eluted proteins (IP) were prepared for western blotting by adding 20  $\mu$ L of loading buffer ( $\times 5$ ) and 5  $\mu$ L of 1 M Tris-HCl pH 10.

Irreversible crosslinking of the antibody to the Sepharose beads was performed after 1 h of incubation at RT of the antibody with protein A Sepharose beads, incubating the beads with 500  $\mu$ L of dimethyl pimelimidate (DMP, Pierce) for 30 min at RT. Next, the columns were washed four times with 500  $\mu$ L of  $\times 1$  TBS, four times with 500  $\mu$ L of 0.2 M glycine pH 2.5 and three times more with  $\times 1$  TBS. Next, the columns were incubated with the protein lysates to perform immunoprecipitation following the above-described protocol.

Protein samples (50  $\mu$ g), SN and IP were boiled in Laemmli SDS loading buffer and separated by 10% SDS-PAGE. For the nondenaturing technique, no boiling step was applied, and the SDS-PAGE gel was 8%. Next, samples were transferred to nitrocellulose membranes (Immobilon-P, Millipore) and blocked in 0.2% Tween-20-PBS supplemented with 5% dry milk before immunoreaction. Filters were immunoblotted with antibodies against Kv $\beta$ 1.1 (1/1,000, Neuromab), Kv $\beta$ 2.1 (1/1,000, Neuromab), Clathrin (1/1,000, BD Transduction) or Caveolin (1/1,000, BD transduction). Finally, the filters were washed with 0.05% Tween 20 PBS and incubated with horseradish peroxidase-conjugated secondary antibodies (Bio-Rad).

## Confocal Microscopy and Image Analysis

For confocal microscopy, cells were seeded on poly-lysine-coated coverslips and transfected 24 h later. The next day, the cells were quickly washed twice, fixed with 4% paraformaldehyde for 10 min, and washed three times for 5 min with PBS-K+. Finally, coverslips were mounted on microscope slides (Acefesa) with house Mowiol mounting media. Coverslips were dried at RT at least 1 day before imaging.

The fluorescence resonance energy transfer (FRET) via the acceptor photobleaching technique was measured in a discrete region of interest (ROI). Fluorescent proteins from fixed cells were excited with the 458 nm or the 514 nm lines using low excitation intensities. Next, 475–495 nm bandpass and  $>530$  nm longpass emission filters were applied. The YFP was bleached using maximum laser power with a yield of approximately 80% acceptor bleaching. After photobleaching of the acceptor, images of the donors and acceptors were captured. The FRET efficiency was calculated using the equation.

$$\left[ \frac{(F_{\text{CFPafter}} - F_{\text{CFPbefore}})}{F_{\text{CFPafter}}} \right] \times 100$$
, where  $F_{\text{CFPafter}}$  and  $F_{\text{CFPbefore}}$  are the fluorescence of the donor after and before bleaching, respectively. The loss of fluorescence as a result of the scans was corrected by measuring the CFP intensity in the unbleached part of the cell. All images were acquired with a Leica

TCS SL laser scanning confocal spectral microscope (Leica Microsystems) equipped with argon and helium–neon lasers. All experiments were performed with a  $\times 63$  oil-immersion objective lens NA 1.32. All offline image analyses were performed using ImageJ software.

## Cell Unroofing Preparations

HEK-293 cells were seeded in poly-D-lysine-treated glass coverslips. Twenty-four hours after transfection, they were cooled on ice for 5 min and washed twice in PBS without  $\text{K}^+$ . Next, the samples were incubated for 5 min in KHMgE buffer (70 mM KCl, 30 mM HEPES, 5 mM  $\text{MgCl}_2$ , 3 mM EGTA, pH 7.5) diluted three times and then gently washed with nondiluted KHMgE to induce hypotonic shock. Burst cells were removed from the coverslip by intensively pipetting up and down. After two washes with KHMgE buffer, only membrane sheets remained attached. Preparations were fixed and mounted as previously described (Oliveras et al., 2020).

## Lipid Raft Isolation

Low density Triton-insoluble complexes were isolated as previously described (Martinez-Marmol et al., 2008) from HEK-293 cells transiently transfected with Kv $\beta$ 1.1CFP and Kv $\beta$ 2.1CFP. Cells were homogenized in 1 ml of 1% Triton X-100, and sucrose was added to a final concentration of 40%. A 5–30% linear sucrose gradient was layered on top and further centrifuged ( $\times 390,000$  g) for 20–22 h at  $4^{\circ}\text{C}$  in a Beckman SW41Ti rotor. Gradient fractions (1 ml) were sequentially collected from the top and analyzed by western blotting.

## Spectral Lux-Fluorescence Resonance Energy Transfer Analysis in Living Cells

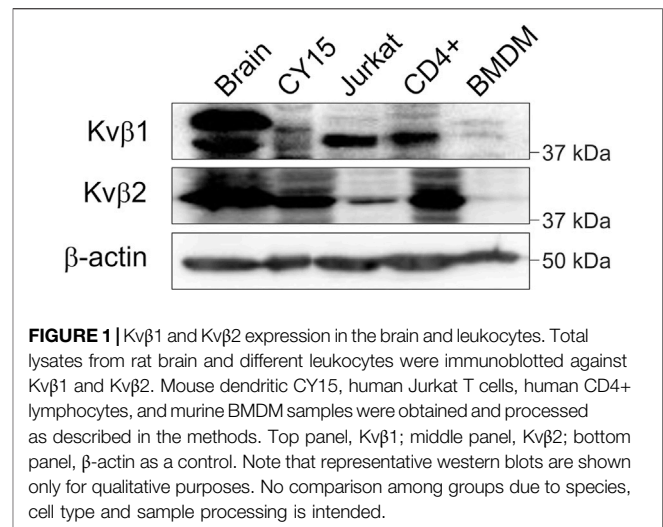
Linear unmixing FRET (lux-FRET) described in (Włodarczyk et al., 2008; Prasad et al., 2013) is a quantitative spectral FRET approach, based on two excitations, preferentially but not necessary where donor and acceptor are best excited, respectively. Lux-FRET treats the variety of possible distances, i.e., FRET states, of donor and acceptor as superposition of free donor and acceptor, and DA complexes. Since lux-FRET is based on spectral unmixing, references of donor only and acceptor only are required. Furthermore, like in other spectral FRET approaches, lux-FRET requires one tandem construct with a fixed one-to-one stoichiometry of donor and acceptor fluorophore. Because the calibration of the tandem construct is independent of the FRET efficiency, the information about the FRET efficiency of the tandem construct is not necessary. With the knowledge of the fluorescence quantum yield of the donor and acceptor fluorophores, lux-FRET is able to deduce the apparent FRET efficiencies  $E_{\text{FD}}$  and  $E_{\text{FA}}$ , where  $f_{\text{D}} = \frac{[\text{DA}]}{[\text{D}^*]}$  and  $f_{\text{A}} = \frac{[\text{DA}]}{[\text{A}^*]}$  are the fractions of donors and acceptors in complexes, respectively; the donor molar fraction ( $x_{\text{D}} = \frac{[\text{D}^*]}{[\text{D}^*] + [\text{A}^*]}$ ); and the total donor (D) and acceptor (A) quantities,  $[\text{D}^*]$  and  $[\text{A}^*]$ , scaled to the reference concentrations. For that, HEK-293 cells were cotransfected with Kv $\beta$ 1.1YFP and Kv $\beta$ 2.1CFP. Twenty-four

hours after transfection, the cells were resuspended in PBS. All lux-FRET measurements were recorded with the fluorescence spectrometer Fluorog-3.22 (Horiba) equipped with a xenon lamp (450 W, 950 V) and two double monochromators. Following configuration and settings were used: 5-mm pathway quartz cuvettes at 37°C in “front face” arrangement, dual excitation 440 and 488 nm, with emission spectra 450–600 nm and 500–600 nm, respectively, 0.5 s integration time. The spectral contributions from light scattering and nonspecific fluorescence of the cells were taken into account by subtracting the emission spectra of non-transfected cells (background) from each measured spectrum. Before the measurements, the spectrofluorometer was calibrated for the xenon lamp spectrum and Raman scattering peak position. To determine the apparent FRET efficiency for Kv $\beta$ 1.1 and Kv $\beta$ 2.1, we used a method described in detail previously (Renner et al., 2012; Prasad et al., 2013)). In short, we obtained relative excitation strengths  $r^{ex,1}$  and  $r^{ex,2}$  of the donor and acceptor from cells expressing, e.g., Kv $\beta$ 1.1CFP or Kv $\beta$ 2.1YFP only and did a non-negative linear unmixing with the corresponding characteristic, the Mock and the Raman spectrum. In the same way we received the donor and acceptor contributions  $\delta^i$  and  $\alpha^i$ , for both excitations  $i$  from co-expressions of donor and acceptor of various relative expression levels. The relative experimental donor to acceptor brightness  $R_{TC} = \frac{\alpha_{TC}^1 \cdot r^{ex,2} - \alpha_{TC}^2 \cdot r^{ex,1}}{\Delta r \cdot \delta^1 + \Delta \alpha_{TC}}$ , with  $\Delta r = r^{ex,2} - r^{ex,1}$  and  $\Delta \alpha = \alpha^2 - \alpha^1$ , required for further calculations, we obtained from a tandem construct TC with one-to-one stoichiometry of donor and acceptor. From that, we calculated the total concentration ratio  $[A^t]/[D^t] = \frac{\alpha^1 \cdot r^{ex,2} - \alpha^2 \cdot r^{ex,1}}{R_{TC} \cdot (\Delta r \cdot \delta^1 + \Delta \alpha)}$  of the donor and acceptor, the donor molar fraction ( $x_D$ )  $x_D = \frac{[D^t]}{[D^t] + [A^t]} = 1 / \frac{1 + [A^t]/[D^t]}{1}$  and the apparent FRET efficiencies  $Ef_D = \frac{\Delta \alpha}{\Delta r \cdot \delta^1 + \Delta \alpha}$  and  $Ef_A = R_{TC} \cdot \frac{\Delta \alpha}{\alpha^1 \cdot r^{ex,2} - \alpha^2 \cdot r^{ex,1}}$  (Włodarczyk et al., 2008). The model characterizing apparent FRET efficiency ( $Ef_D$ ) as a function of donor mole fraction ( $x_D$ ) for oligomeric structures was developed previously (Veatch and Stryer, 1977) following  $Ef_D = E(1 - x_D^{n-1})$ . Fitting this model to experimental data yields the true transfer efficiency ( $E$ ) and provides information about the number of units ( $n$ ) interacting within the oligomeric complex. This model was slightly augmented for use with  $Ef_A = E \frac{x_D}{x_D - 1} (1 - x_D^{n-1})$  (Meyer et al., 2006). The oligomerization model, yielding the total FRET efficiency, the basic subunit formation and the affinity constants, was previously described (Renner et al., 2012).

## RESULTS

### Kv $\beta$ 1.1 and Kv $\beta$ 2.1 are able to Homo- and Heterologomerize

The nervous and immune systems express members of the voltage-gated regulatory subunit family Kv $\beta$  (McCormack et al., 1999; Vicente et al., 2005; Pongs and Schwarz, 2010). Kv $\beta$ 1 and Kv $\beta$ 2 are involved in controlling Kv inactivation and spatial distribution, such as axonal targeting and IS location (Gu



et al., 2003; Beeton et al., 2006; Roig et al., 2022). Therefore, we confirmed that the brain and leukocytes expressed the Kv $\beta$ 1 and Kv $\beta$ 2 subunits. As expected, not only the rat brain but also a wide repertoire of leukocytes, such as mouse CY15 dendritic cells, human Jurkat T cells, human CD4<sup>+</sup> lymphocytes and primary murine bone marrow-derived macrophages (BMDMs), expressed both Kv $\beta$ 1 and Kv $\beta$ 2 regulatory subunits (Figure 1). Therefore, Kv $\beta$ s are ubiquitously expressed within the immune system.

Most of the work related to the Kv $\beta$  family addresses the regulation of Kv channels (Pongs and Schwarz, 2010). Some studies address the modulation, *via* AKR activity, of the  $\alpha$ -subunits. However, scarce information is available on the putative oligomeric formation of Kv $\beta$ s. Evidence indicates that Kv $\beta$ 2, but not Kv $\beta$ 1, forms complexes. Kv $\beta$ 1 controls channel activity in a concentration-dependent manner, and Kv $\beta$ 2, by trapping Kv $\beta$ 1 in those complexes, could impair its function on the  $\alpha$ -subunits (Xu and Li, 1997; Xu et al., 1998). Structural studies indicate a prevalent tetrameric composition for the Kv $\beta$ 2 complexes (Gulbis et al., 1999; van Huizen et al., 1999). Although evidence demonstrates that Kv $\beta$ 2.1 forms homo- and heteromers with Kv $\beta$ 1, no Kv $\beta$ 1 oligomers have been detected in the absence of Kv channels. In this scenario, coimmunoprecipitation assays were performed in HEK cells transfected with Kv $\beta$ 1.1CFP/Kv $\beta$ 1.1, Kv $\beta$ 2.1CFP/Kv $\beta$ 2.1 and Kv $\beta$ 1.1CFP/Kv $\beta$ 2.1. Our data showed that in the absence of any Kv  $\alpha$  subunit, Kv $\beta$ 2.1, as well as Kv $\beta$ 1.1, showed significant homo- and heterocoimmunoprecipitation (Figures 2A–C).

To explore further oligomeric associations, a series of FRET experiments were performed (see representative Kv $\beta$ 1.1CFP/Kv $\beta$ 2.1YFP in Figure 2D). Cells were transfected with Kv $\beta$ sCFP (Kv $\beta$ 1.1CFP, Figure 2Da) and Kv $\beta$ sYFP (Kv $\beta$ 2.1YFP, Figure 2Db) used as donor and acceptor fluorophores, respectively. Positive colocalization spots (Figure 2Dc) were subject to the acceptor bleach (white square in Figure 2Dd). FRET values confirmed that, similar to the tetrameric Kv1.3 channel (positive control), Kv $\beta$ 1.1CFP/

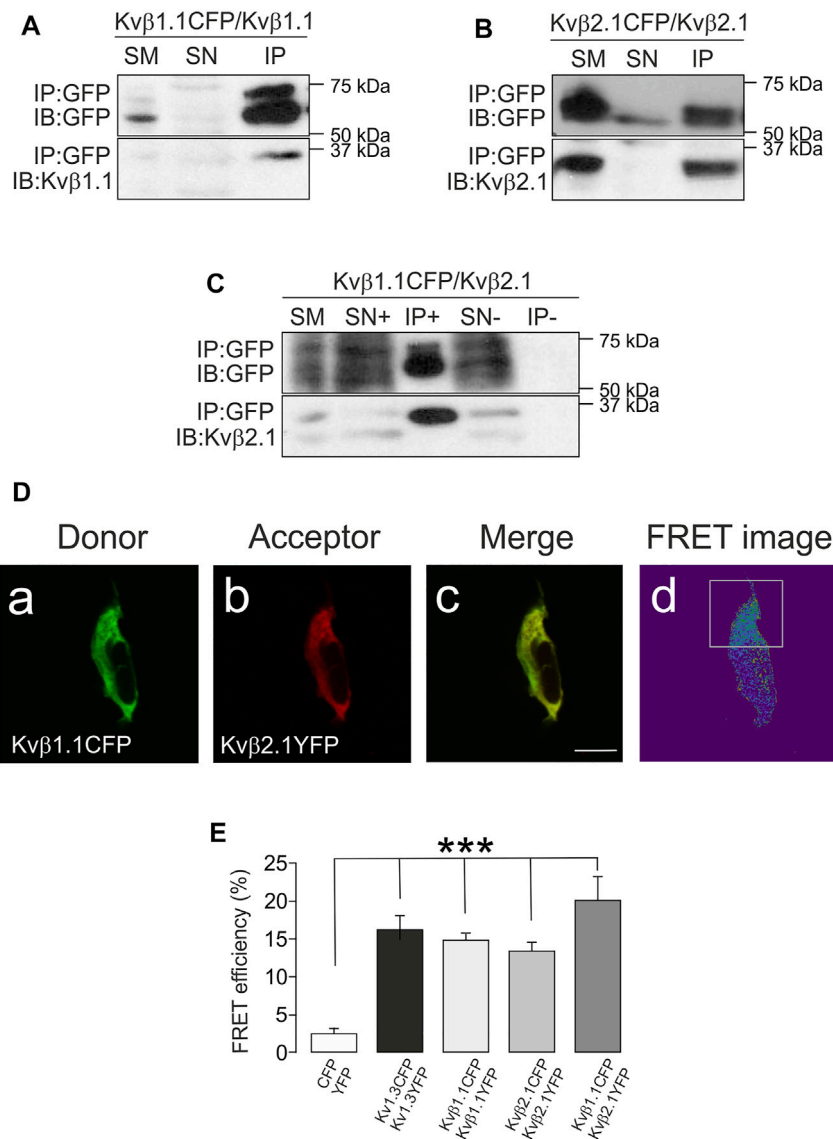


**FIGURE 2** | Kvb1.1 and Kvb2.1 form oligomers. HEK 293 cells were transfected with Kvb1.1 and Kvb2.1. **(A)** Coimmunoprecipitation assay against Kvb1.1CFP in the presence of Kvb1.1. **(B)** Coimmunoprecipitation assay against Kvb2.1CFP in the presence of Kvb2.1. **(C)** Coimmunoprecipitation assay against Kvb1.1CFP in the presence of Kvb2.1. **(C)**. Top panels: immunoprecipitation (IP) of CFP and immunoblot (IB) against CFP. Bottom panels: IB against Kvb1.1 **(A)** and Kvb2.1 **(B,C)**. SM: starting material. SN+: supernatant in the presence of the antibody. IP+: immunoprecipitation in the presence of the antibody. SN-: supernatant in the absence of the antibody. IP-: immunoprecipitation in the absence of the antibody. **(D)** Kvb1.1 and Kvb2.1 form homo- and hetero-oligomers. Representative image of Kvb1.1 and Kvb2.1 cotransfection. **(Da)** Donor, Kvb1.1CFP; **(Db)** Acceptor, Kvb2.1 YFP; **(Dc)** merge, yellow indicates colocalization; **(Dd)** FRET image obtained from the relationship between the donor prebleach versus postbleach after acceptor photobleaching. The white square highlights the bleached section. The bar represents 20  $\mu$ m. **(E)** FRET efficiencies (%) calculated from the acceptor photobleaching experiments. Values are the mean  $\pm$  SE of >30 cells. \*\*\* $p$  < 0.01 vs. CFP/YFP negative control (Student's  $t$  test).

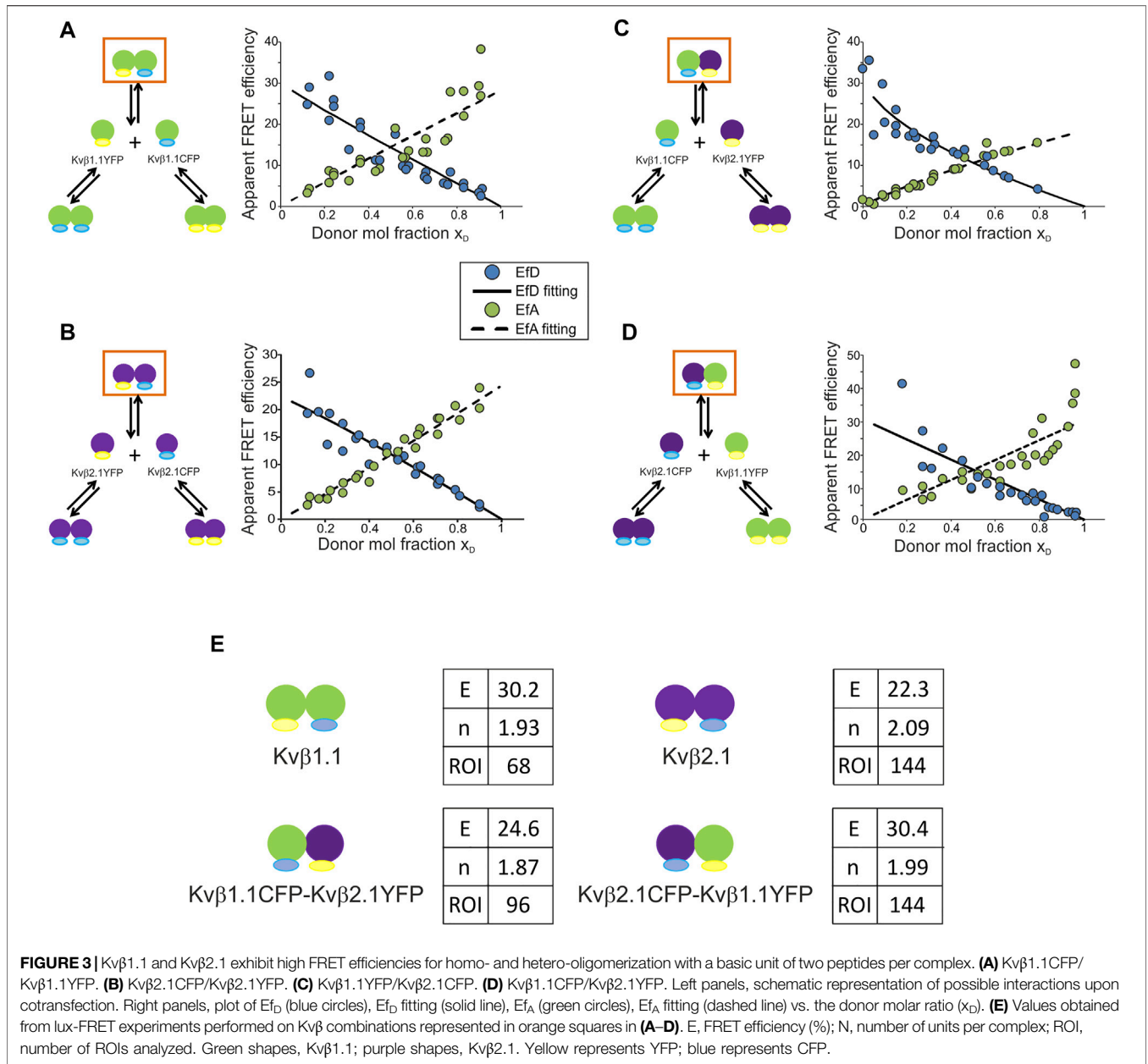
Kvb1.1YFP, Kvb2.1CFP/Kvb2.1YFP and Kvb1.1CFP/Kvb2.1YFP form homo- and hetero-oligomeric complexes (**Figure 2E**).

## Kvb Homo- and Hetero-Oligomerization Affinities are Similar

Evidence suggests a preferred configuration of Kv $\beta$  complexes containing Kvb2. However, our data indicated that Kvb1 would also form oligomers in the absence of  $\alpha$ -units. To

decipher the affinity of the Kv $\beta$  complexes, we applied the linear unmixing FRET (lux-FRET) technique, which provides the apparent donor and acceptor FRET efficiencies, stoichiometry and affinity constants of interactions (Wlodarczyk et al., 2008). Experiments were performed in cell suspensions transfected with different donor molar ratios (**Figure 3**).

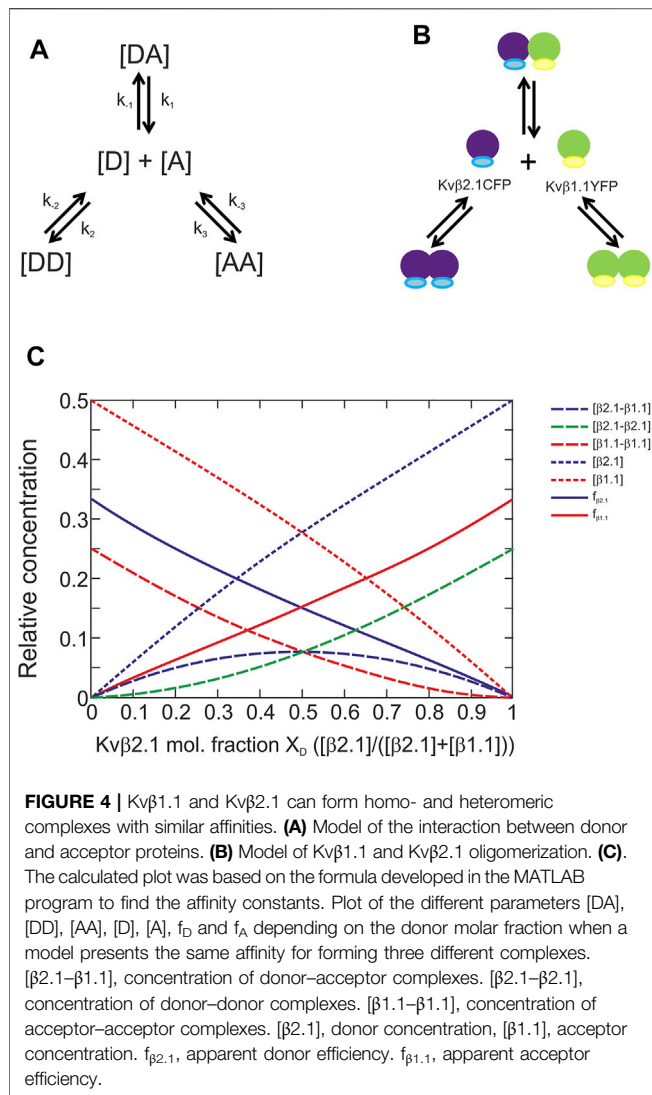
Coexpression of Kvb1.1CFP/Kvb1.1YFP raised three different complexes: homomeric Kvb1.1CFP, homomeric Kvb1.1YFP and



Kvβ1.1CFP/Kvβ1.1YFP heteromers. FRET confirmed the formation of heteromeric complexes (orange box in **Figure 3A**). In this case, lux-FRET values demonstrated an inverse correlation between the FRET efficiency of the donor ( $E_{FD}$ ) and the donor molar fraction (solid line, **Figure 3A**). The apparent FRET efficiency of the acceptor ( $E_{FA}$ ) was the opposite. Thus, the higher the donor molar fraction is, the higher the apparent FRET efficiency (dashed line, **Figure 3A**). From these data, the FRET efficiency (E) and stoichiometry (N) of the complex were calculated. The FRET efficiency was 30.2%, and the basic unit involved two Kvβ1.1 subunits ( $n = 1.93$ ) (**Figure 3E**). Kvβ2.1CFP/Kvβ2.1YFP exhibited a similar

pattern (**Figure 3B**), showing 22.3% FRET efficiency and a basic unit of two Kvβ2.1 peptides ( $n = 2.09$ ) (**Figure 3E**).

We next analyzed Kvβ1.1CFP/Kvβ2.1YFP and reciprocal Kvβ2.1CFP/Kvβ1.1YFP (**Figures 3C,D**). The Kvβ1.1CFP/Kvβ2.1YFP plot shifted to a lower  $x_D$  due to a slightly lower expression of Kvβ1.1CFP compared with Kvβ2.1YFP (**Figure 3C**). In this case, the calculated FRET efficiency was 32.5% with a basic unit of two proteins ( $n = 1.88$ ) per complex (**Figure 3E**). Kvβ2.1CFP/Kvβ1.1YFP shifted in the opposite  $x_D$  direction due to the same effect by the lowest Kvβ2.1CFP expression (**Figure 3D**). In this context, Kvβ2.1 again presented a value of a basic unit of two ( $n = 1.99$ ) and a FRET of 30.4% (**Figure 3E**).



The calculation of the affinity constants was based on the model presented in **Figure 4A**. The mixture between a donor and an acceptor yields three different complexes. Each complex is formed to a greater or lesser extent depending on their affinity constants (Renner et al., 2012). This model was implemented to solve the Kvβ1.1/Kvβ2.1 affinity (**Figure 4B**). The system relies on previous evaluation of homomeric forms. Next, the different affinity constants could be defined by using the following formula.

$$\left(-K_{DD} + \sqrt{K_{DD}^2 + 8K_{DD}([D]_i - [DA])}\right) \times \left(-K_{AA} + \sqrt{K_{AA}^2 + 8K_{AA}([A]_i - [DA])}\right) = 16K_{DA}[DA]$$

Our abovementioned data were concomitant with the plot in **Figure 4C**, which suggests that the 3 affinity constants ( $k$ ) in our model were similar. Thus, unlike 5-HT receptors, the absence of tilted ends in our plots indicated no differences in affinities, and therefore no preferences, between Kvβ1.1 and Kvβ2.1 forming homo- and hetero-oligomers (Renner et al., 2012).

## Kvβ1.1 and Kvβ2.1 Form Tetramers by Dimer Dimerization

Our data established that the basic unit for oligomerization was two peptides. This result implies that two different possibilities for the complex dynamics existed: 1) Kvβs form dimers; 2) these dimers oligomerize to form tetrameric structures (**Figure 5A**). Our results also indicated no trimeric structures (**Figure 3E**). Because Kvβ2.1 forms tetramers in the absence of the  $\alpha$ -subunit, we wondered whether this also applies to the Kvβ1.1 subunit. Semidenaturing gel electrophoresis was implemented in HEK cells transfected with Kvβ1.1CFP and Kvβ2.1CFP (van Huizen et al., 1999). Monomeric structures were detected in all four conditions tested, but unlike YFP-transfected cells (**Figure 5B**), dimers and tetramers were found in Kv1.3YFP, Kvβ1.1YFP and Kvβ2.1YFP (**Figures 5C,D**). Kv1.3YFP was used as a control because of its tetrameric architecture. Thus, monomers, some dimers and tetramers were clearly visible (**Figure 5C**). Similarly, Kvβ1.1 and Kvβ2.1 analysis triggered monomeric, dimeric and tetrameric forms (**Figure 5D**). Therefore, in agreement with the lux-FRET data, no trimeric complexes were detected. Taken together, our data showed that both Kvβ1.1 and Kvβ2.1 could form tetramers by a dimeric interaction.

## Surface Spatial Localization of Oligomeric Kvβ Compositions

Kvβ1.1 and Kvβ2.1 target the membrane surface, but only Kvβ2.1 is located in lipid rafts, independent of Kv1.3, in a palmitoylation-dependent manner (Roig et al., 2022). This spatial localization is crucial because Kvβ2.1 clusters at the IS during the immune system response (Beeton et al., 2006; Roig et al., 2022). Therefore, putative oligomeric Kvβ compositions, whose stoichiometry would depend on variable protein expression, could fine-tune leukocyte physiology. In this context, we sought to decipher whether Kvβ subunits target the plasma membrane in the absence of K $\alpha$  subunits as homo- or hetero-oligomeric complexes. CUPs were purified from HEK transfected cells, and FRET between Kvβs was analyzed (**Figure 6**). Only the negative CFP-YFP control was measured in a whole-cell configuration because CFP-YFP is a soluble peptide (**Figures 6A–C**). The tetrameric Kv1.3CFP/Kv1.3YFP channel was used as a positive control (**Figures 6D–F**). The FRET efficiency values of Kvβ1.1CFP/Kvβ1.1YFP (**Figures 6G–I**), Kvβ2.1CFP/Kvβ2.1YFP (**Figure 6J–L**) and Kvβ1.1CFP/Kvβ2.1YFP (**Figures 6M–O**) were clearly positive (**Figure 6P**). These results demonstrated that homo- and hetero-oligomeric Kvβ structures target the plasma membrane.

Kvβ2.1, but not Kvβ1.1, is located in lipid rafts (Roig et al., 2022). Because the Kvβ affinity for homo- and heteromultimerization was similar, we investigated whether Kvβ2.1 and Kvβ1.1 would target rafts in a hetero-oligomeric configuration. Low-buoyancy membrane fractions from transfected HEK-293 cells were analyzed. While Kvβ1.1 was not present in raft domains (**Figure 7A**), Kvβ2.1 exhibited partial localization in these fractions (**Figure 7B**). Coexpression of both subunits (Kvβ1.1/Kvβ2.1) triggered

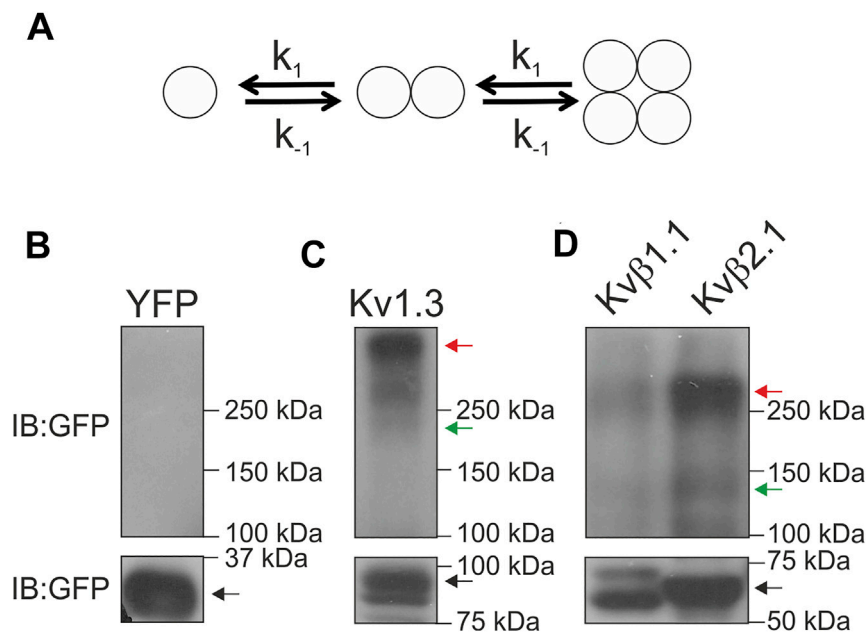


**FIGURE 5** | Kv $\beta$ 1.1 and Kv $\beta$ 2.1 form dimeric and tetrameric structures. **(A)** Model representing the two putative options for Kv $\beta$  oligomerization. Kv $\beta$  forms dimers, and Kv $\beta$  forms tetrameric structures by association. The affinity constant ( $k$ ) for every step would be the same in all conditions. **(B–D)** HEK 293 cells were transfected with YFP, Kv1.3YFP, Kv $\beta$ 1.1YFP and Kv $\beta$ 2.1YFP. Total lysates were analyzed in semidenaturing conditions. **(B)** YFP, **(C)** Kv1.3YFP, **(D)** Kv $\beta$ 1.1YFP and Kv $\beta$ 2.1YFP. Immunoblots (IB) were performed with an anti-GFP antibody. Blots were split into two for low- and high-molecular-weight forms for better visualization. The black arrow indicates monomeric forms. The green arrow indicates dimeric forms. The red arrow highlights tetrameric forms.

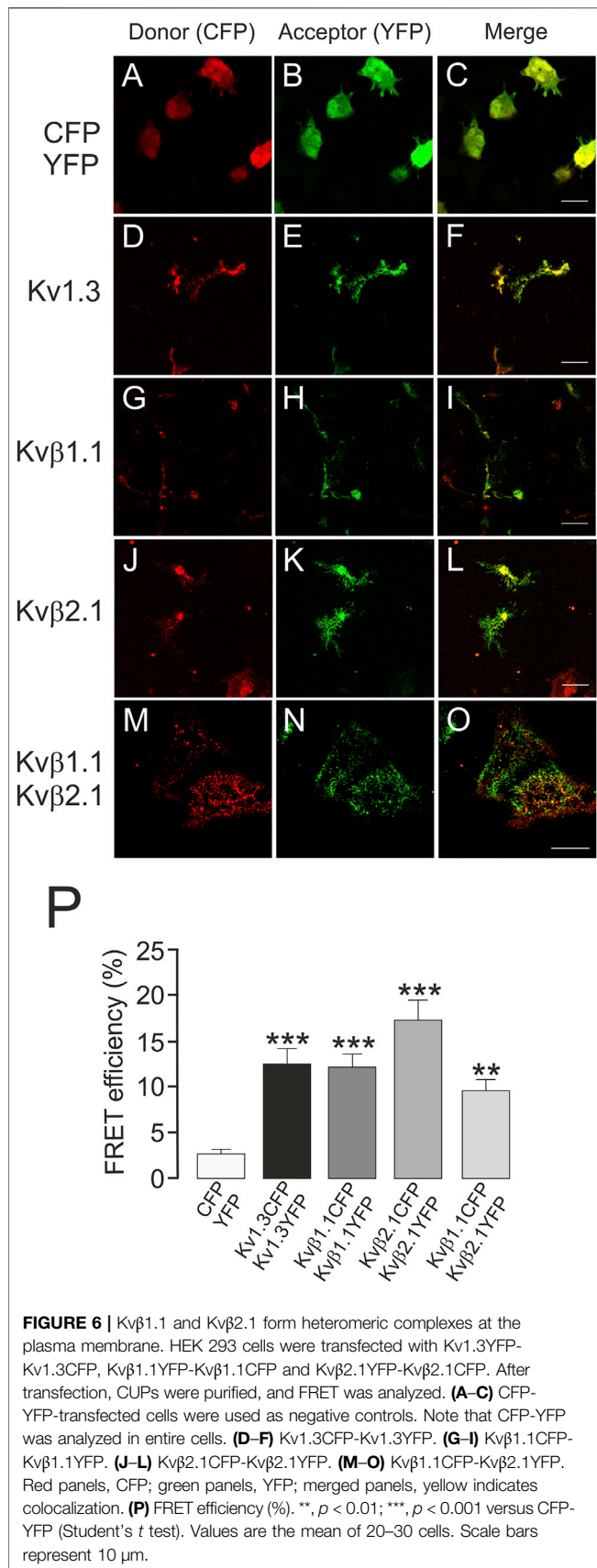
Kv $\beta$ 2.1 to no longer traffic to raft microdomains (**Figure 7C**). Therefore, Kv $\beta$ 1.1 hetero-oligomerization altered Kv $\beta$ 2.1 membrane localization in lipid rafts.

## DISCUSSION

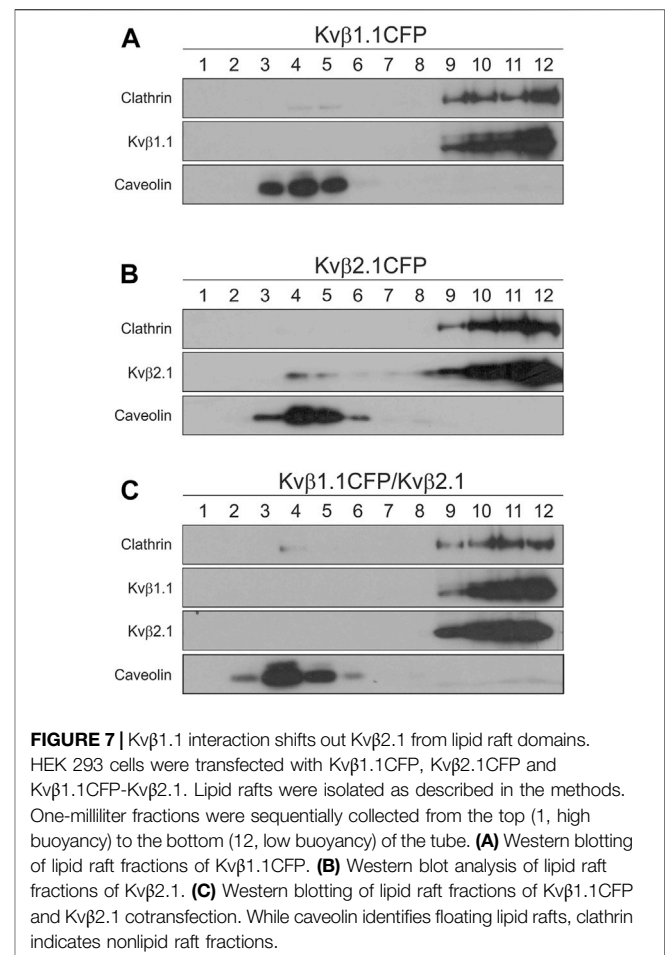
The physiological function of Kv channels is tightly regulated by regulatory  $\beta$  subunits (Pongs and Schwarz, 2010). The composition and stoichiometry of the  $\alpha$ - $\beta$  complex ultimately determine the kinetics and gating of potassium channels as well as their cellular traffic and distribution (Pongs and Schwarz, 2010). We demonstrated that Kv $\beta$ 1.1 and Kv $\beta$ 2.1 form heteromeric complexes. Both peptides present over 85% similarity, and the regions involved in oligomerization are highly conserved. Although the homomeric composition for Kv $\beta$ 2 was described early (Xu et al., 1998; van Huizen et al., 1999), the tetrameric ability of Kv $\beta$ 1 subunits is a subject of debate (Accili et al., 1997). The crystal structure of Kv $\beta$ 2 sustains a tetrameric architecture that was also inferred for Kv $\beta$ 1 (Gulbis et al., 1999). However, hetero-oligomeric complexes always contain Kv $\beta$ 2 (Nystoriak et al., 2017). Our work demonstrates that both Kv $\beta$ s may form homotetramers. The tetramer is generated by dimerization of dimers. Both the homo- and heterotetrameric complexes exhibit similar affinity constants for both Kv $\beta$ s. Therefore, differential abundance of Kv $\beta$ s would shape the stoichiometry. In addition, Kv $\beta$ 2, but not Kv $\beta$ 1, targets lipid raft

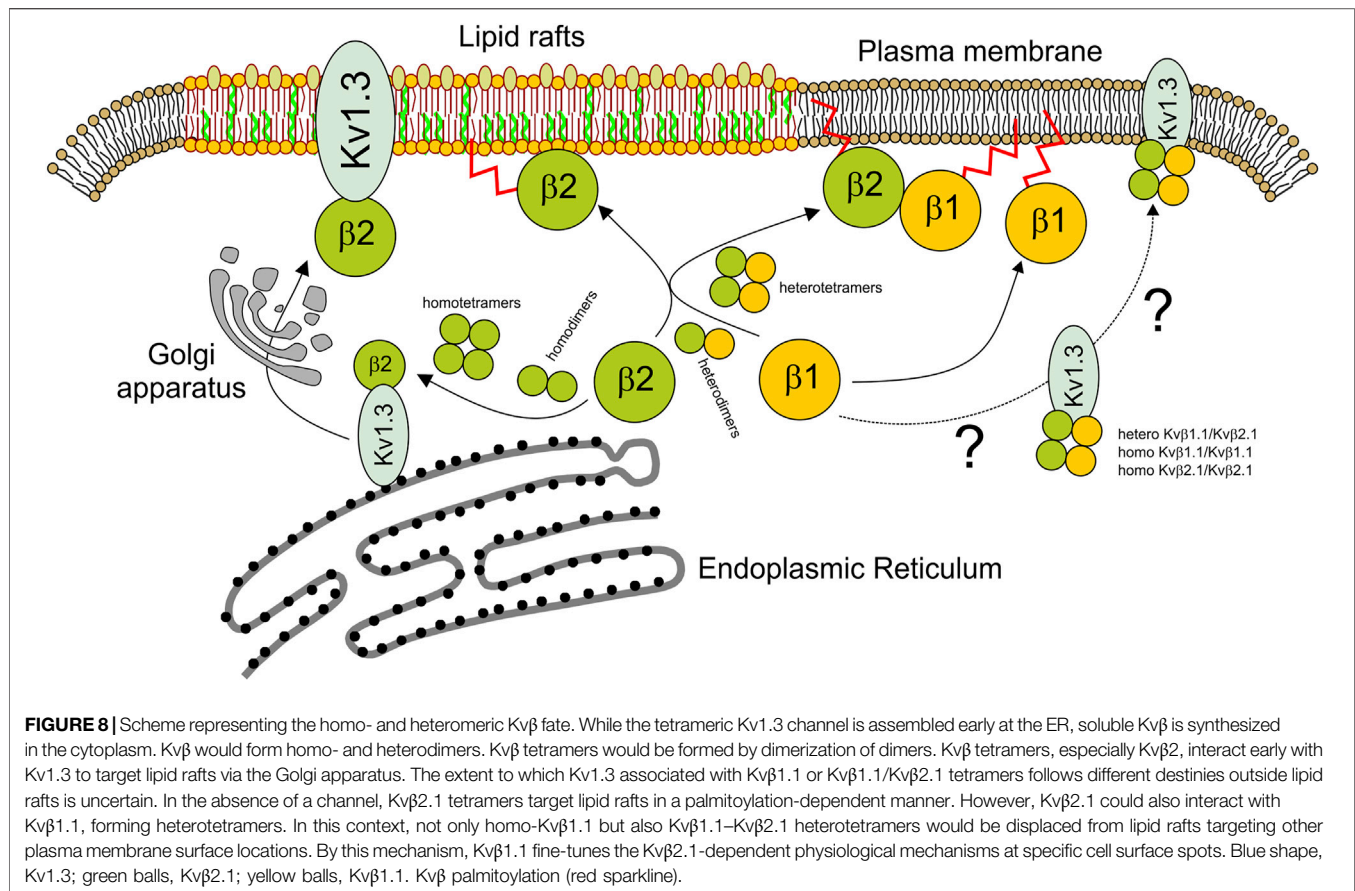
microdomains, and the heteromeric composition of the complex impairs the raft location of the Kv $\beta$ 1/Kv $\beta$ 2 structure. Given that Kv $\beta$ 2 clusters at the IS, which concentrates lipid rafts, participating during the immunological response, the Kv $\beta$ 1 interaction would fine-tune the physiological function by misallocating Kv $\beta$ 2 from these signaling spots (**Figure 8**).

Our study also sheds light on the dynamic formation of Kv $\beta$  complexes. We found that the tetrameric composition Kv $\beta$ s follows two sequential steps: 1) dimeric formation and 2) dimer dimerization to form the final tetrameric configuration. Although early evidence suggested trimeric structures (van Huizen et al., 1999), our results can only be fitted to a sequential dimerization of dimers, which would be in agreement with what was described for Kv $\beta$ 2 homotetramers. Our findings would thereby be concomitant with the oligomerization that Kv  $\alpha$  units undergo to form a conducting entity (Hille, 2001). A putative low oligomerization affinity would explain the negative homomeric Kv $\beta$ 1.1 associations previously documented. In this context, because only Kv $\beta$ 2 forms tetramers, upon elevated expression, homomeric Kv $\beta$ 2 complexes displace Kv $\beta$ 1, impairing its function (Xu and Li, 1997). However, we found that Kv $\beta$ 1.1 formed oligomers with similar affinity, and the same was true for Kv $\beta$ 1/Kv $\beta$ 2 heterotetramerization. In fact, Kv $\beta$ 1/Kv $\beta$ 2 heterooligomers are expressed in coronary arterial myocytes, regulating Kv1.5 fine-tuning of the trafficking and membrane



localization of the channel (Nystoriak et al., 2017). We confirm previous evidence, but our contribution further shows that Kvβ2.1 and Kvβ1.1 form hetero-oligomers with similar affinities in the absence of the Kv channel. Thus, the unique factor governing multiple stoichiometries would be the differential regulation of both Kvβ peptides. In this scenario, the pattern of Kvβ subunit expression in macrophages depends upon proliferation and the mode of activation (Vicente et al., 2005). Therefore, Kv modulation depends on the final composition of the Kvβ heterotetramer architecture. Several proteins exhibit oligomeric composition control depending on the amount of each partner. For instance, ZIP1/ZIP2/ZIP3 are established hetero- and homodimers depending on the expression level upon different insults (Gong et al., 1999; Croci et al., 2003). In this vein, the heterotetrameric Kv1.3/Kv1.5 channel of professional antigen-presenting cells, such as dendritic cells and macrophages, follow the same fate (Vicente et al., 2006; Villalonga et al., 2007; Vallejo-Gracia et al., 2021). Because two different subunits can govern one unique channel, fine-tuning Kvβ concentrations would trigger a repertoire of functional channels (Pongs and Schwarz, 2010).





Homo- and hetero-oligomers of Kv $\beta$ 1.1/Kv $\beta$ 2.1 targeted the membrane surface, but their microdomain localization was different. While Kv $\beta$ 1.1 is associated with the actin cytoskeleton (Nakahira et al., 1998), Kv $\beta$ 2.1 partially resides in lipid rafts (Roig et al., 2022). Both Kv $\beta$  proteins are palmitoylated, and palmitoylation of Kv $\beta$ 2 is crucial for its location in these domains (Roig et al., 2022). This is of physiological relevance because Kv $\beta$ 2 clusters at the IS, which are enriched in lipid rafts, representing an essential hub for signaling during the immune response (Beeton et al., 2006). Kv $\beta$ 2 is situated in the IS, either modulating Kv1.3 or functioning as a hub for protein-protein interactions. Heterooligomeric interactions between Kv $\beta$ 1 and Kv $\beta$ 2 misplace the latter from lipid rafts and impair the function of Kv $\beta$ 2 in these microdomains. In addition, the presence of Kv $\beta$ 1 altered the function of Kv $\beta$ 2 in a concentration-dependent manner. Therefore, the Kv $\beta$ 1 interaction might fine-tune the Kv $\beta$ 2-dependent physiological consequences during the immune response. In addition to regulating Kv channels and cluster protein interactions, Kv $\beta$ s are also AKRs; therefore, redox variations can be sensed (Kilfoil et al., 2013). The different distribution of Kv $\beta$  throughout the cell surface would provide a differential redox sensitivity in different microdomains. Moreover, the diverse affinity for NADPH determines differential spatial triggers. Kv $\beta$ 2 forms part of the signaling complex, which interacts with CD4, Kv1.3, ZIP1/2 and PSD proteins and clusters at the immunological synapse in human

T cells (Beeton et al., 2006; Roig et al., 2022). In addition, within these locations, Kv $\beta$ 2 is regulated by PKC, p56lck and other signaling kinases (Kwak et al., 1999; Wang et al., 2004; Kim et al., 2005; Roepke et al., 2007; Ishii et al., 2013). Therefore, any spatial alteration in the localization of Kv $\beta$ 2, as well as changes in Kv $\beta$ 2-dependent enzymatic functions, such as modulating the Kv1.3 channelosome, surely would have essential consequences for leukocyte physiology.

## DATA AVAILABILITY STATEMENT

The original contributions presented in the study are included in the article/**Supplementary Material**, further inquiries can be directed to the corresponding author.

## ETHICS STATEMENT

The studies involving human participants were reviewed and approved by the Ethics Committee of the Universitat de Barcelona and the Banc de Sang i Teixits de Catalunya (BST). Institutional Review Board (IRB00003099). All procedures followed the rules of the Declaration of Helsinki Guidelines. The patients/participants provided their written informed consent to participate in this study. The animal study was

reviewed and approved by Universitat de Barcelona in accordance with the European Community Council Directive 86/609 EEC.

## AUTHORS' CONTRIBUTIONS

SR, SC, and AZ performed experiments. SR, AZ, EP and AF designed the experiments. SR, AZ and AF wrote the manuscript. EP and AF directed the work. All the authors discussed the findings and revised the final version of the paper.

## FUNDING

Supported by the Ministerio de Ciencia e Innovación (MICINN/AEI), Spain (PID 2020-112647RB-I00 and 10.13039/501100011033)

## REFERENCES

- Accili, E. A., Kiehn, J., Wible, B. A., and Brown, A. M. (1997). Interactions Among Inactivating and Noninactivating Kv $\beta$  Subunits, and Kva1.2, Produce Potassium Currents with Intermediate Inactivation. *J. Biol. Chem.* 272 (45), 28232–28236. doi:10.1074/jbc.272.45.28232
- Beeton, C., Wulff, H., Standifer, N. E., Azam, P., Mullen, K. M., Pennington, M. W., et al. (2006). Kv1.3 Channels Are a Therapeutic Target for T Cell-Mediated Autoimmune Diseases. *Proc. Natl. Acad. Sci. U.S.A.* 103 (46), 17414–17419. doi:10.1073/pnas.0605136103
- Capera, J., Pérez-Verdaguer, M., Peruzzo, R., Navarro-Pérez, M., Martínez-Pinna, J., Alberola-Die, A., et al. (2021). A Novel Mitochondrial Kv1.3-caveolin axis Controls Cell Survival and Apoptosis. *Elife* 10. doi:10.7554/eLife.69099
- Croci, C., Brandstätter, J. H., and Enz, R. (2003). ZIP3, a New Splice Variant of the PKC- $\zeta$ -Interacting Protein Family, Binds to GABAC Receptors, PKC- $\zeta$ , and Kv $\beta$ 2. *J. Biol. Chem.* 278 (8), 6128–6135. doi:10.1074/jbc.M205162200
- Gong, J., Xu, J., Bezanilla, M., Huizen, R. v., Derin, R., and Li, M. (1999). Differential Stimulation of PKC Phosphorylation of Potassium Channels by ZIP1 and ZIP2. *Science* 285 (5433), 1565–1569. doi:10.1126/science.285.5433.1565
- Gu, C., Jan, Y. N., and Jan, L. Y. (2003). A Conserved Domain in Axonal Targeting of Kv1 (Shaker) Voltage-Gated Potassium Channels. *Science* 301 (5633), 646–649. doi:10.1126/science.1086998
- Gulbis, J. M., Mann, S., and MacKinnon, R. (1999). Structure of a Voltage-dependent K $^{+}$  Channel  $\beta$  Subunit. *Cell* 97 (7), 943–952. doi:10.1016/s0092-8674(00)80805-3
- Heinemann, S. H., Rettig, J., Wunder, F., and Pongs, O. (1995). Molecular and Functional Characterization of a Rat Brain Kv Beta 3 Potassium Channel Subunit. *FEBS Lett.* 377 (3), 383–389. doi:10.1016/0014-5793(95)01377-6
- Hille, B. (2001). *Ion Channels of Excitable Membranes*. Sunderland, Massachusetts: Sinauer Associates.
- Hyndman, D., Bauman, D. R., Heredia, V. V., and Penning, T. M. (2003). The Aldo-Keto Reductase Superfamily Homepage. *Chemico-Biological Interact.* 143–144, 621–631. doi:10.1016/s0009-2797(02)00193-x
- Ishii, T., Warabi, E., Siow, R. C. M., and Mann, G. E. (2013). Sequestosome1/p62: a Regulator of Redox-Sensitive Voltage-Activated Potassium Channels, Arterial Remodeling, Inflammation, and Neurite Outgrowth. *Free Radic. Biol. Med.* 65, 102–116. doi:10.1016/j.freeradbiomed.2013.06.019
- Kilfoil, P. J., Tipparaju, S. M., Barski, O. A., and Bhatnagar, A. (2013). Regulation of Ion Channels by Pyridine Nucleotides. *Circ. Res.* 112 (4), 721–741. doi:10.1161/CIRCRESAHA.111.247940
- Kim, Y., Park, M.-K., Uhm, D.-Y., Shin, J., and Chung, S. (2005). Modulation of Delayed Rectifier Potassium Channels by  $\alpha$ 1-adrenergic Activation via Protein Kinase C  $\zeta$  and P62 in PC12 Cells. *Neurosci. Lett.* 387 (1), 43–48. doi:10.1016/j.neulet.2005.07.016

and European Regional Development Fund (FEDER). EP was supported by the Deutsche Forschungsgemeinschaft (DFG) grant PO732. AZ was supported by the DFG grant AZ994.

## ACKNOWLEDGMENTS

SR and SC contributed equally and held fellowships from MICINN. The English editorial assistance of the American Journal Experts is also acknowledged.

## SUPPLEMENTARY MATERIAL

The Supplementary Material for this article can be found online at: <https://www.frontiersin.org/articles/10.3389/fphys.2022.930769/full#supplementary-material>

- Kwak, Y.-G., Hu, N., Wei, J., George, A. L., Jr., Grobaski, T. D., Tamkun, M. M., et al. (1999). Protein Kinase A Phosphorylation Alters Kv $\beta$ 1.3 Subunit-Mediated Inactivation of the Kv1.5 Potassium Channel. *J. Biol. Chem.* 274 (20), 13928–13932. doi:10.1074/jbc.274.20.13928
- Leicher, T., Roeper, J., Weber, K., Wang, X., and Pongs, O. (1996). Structural and Functional Characterization of Human Potassium Channel Subunit  $\beta$ 1 (KCNA1B). *Neuropharmacology* 35 (7), 787–795. doi:10.1016/0028-3908(96)00133-5
- Martínez-Mármol, R., Villalonga, N., Solé, L., Vicente, R., Tamkun, M. M., Soler, C., et al. (2008). Multiple Kv1.5 Targeting to Membrane Surface Microdomains. *J. Cell. Physiol.* 217 (3), 667–673. doi:10.1002/jcp.21538
- McCormack, T., McCormack, K., Nadal, M. S., Vieira, E., Ozaita, A., and Rudy, B. (1999). The Effects of Shaker  $\beta$ -Subunits on the Human Lymphocyte K $^{+}$  Channel Kv1.3. *J. Biol. Chem.* 274 (29), 20123–20126. doi:10.1074/jbc.274.29.20123
- Meyer, B. H., Segura, J.-M., Martínez, K. L., Hovius, R., George, N., Johnsson, K., et al. (2006). FRET Imaging Reveals that Functional Neurokinin-1 Receptors Are Monomeric and Reside in Membrane Microdomains of Live Cells. *Proc. Natl. Acad. Sci. U.S.A.* 103 (7), 2138–2143. doi:10.1073/pnas.0507686103
- Nakahira, K., Matos, M. F., and Trimmer, J. S. (1998). Differential Interaction of Voltage-Gated K $^{+}$  Channel  $\beta$ -Subunits with Cytoskeleton Is Mediated by Unique Amino Terminal Domains. *Jmn* 11 (3), 199–208. doi:10.1385/JMN:11:3:199
- Nystoriak, M. A., Zhang, D., Jagatheesan, G., and Bhatnagar, A. (2017). Heteromeric Complexes of Aldo-Keto Reductase Auxiliary K V  $\beta$  Subunits (AKR6A) Regulate Sarcolemmal Localization of K V 1.5 in Coronary Arterial Myocytes. *Chemico-Biological Interact.* 276, 210–217. doi:10.1016/j.cbi.2017.03.011
- Oliveras, A., Serrano-Novillo, C., Moreno, C., de la Cruz, A., Valenzuela, C., Soeller, C., et al. (2020). The Unconventional Biogenesis of Kv7.1-KCNE1 Complexes. *Sci. Adv.* 6 (14), eaay4472. doi:10.1126/sciadv.aay4472
- Parcej, D. N., Scott, V. E. S., and Dolly, J. O. (1992). Oligomeric Properties of  $\alpha$ -Dendrotoxin-Sensitive Potassium Ion Channels Purified from Bovine Brain. *Biochemistry* 31 (45), 11084–11088. doi:10.1021/bi00160a018
- Pongs, O., and Schwarz, J. R. (2010). Ancillary Subunits Associated with Voltage-dependent K $^{+}$  Channels. *Physiol. Rev.* 90 (2), 755–796. doi:10.1152/physrev.00020.2009
- Prasad, S., Zeug, A., and Ponimaskin, E. (2013). Analysis of Receptor-Receptor Interaction by Combined Application of FRET and Microscopy. *Methods Cell Biol.* 117, 243–265. doi:10.1016/B978-0-12-408143-7.00014-1
- Renner, U., Zeug, A., Woehler, A., Niebert, M., Dityatev, A., Dityateva, G., et al. (2012). Heterodimerization of Serotonin Receptors 5-HT1A and 5-HT7 Differentially Regulates Receptor Signalling and Trafficking. *J. Cell Sci.* 125 (Pt 10), 2486–2499. doi:10.1242/jcs.101337
- Roeper, T. A., Malyala, A., Bosch, M. A., Kelly, M. J., and Rønnekleiv, O. K. (2007). Estrogen Regulation of Genes Important for K $^{+}$  Channel Signaling in the Arcuate Nucleus. *Endocrinology* 148 (10), 4937–4951. doi:10.1210/en.2007-0605

- Roig, S. R., Cassinelli, S., Navarro-Pérez, M., Pérez-Verdaguer, M., Estadella, I., Capera, J., et al. (2022). S-acylation-dependent Membrane Microdomain Localization of the Regulatory Kv $\beta$ 2.1 Subunit. *Cell. Mol. Life Sci.* 79 (5), 230. doi:10.1007/s00018-022-04269-3
- Shi, G., Nakahira, K., Hammond, S., Rhodes, K. J., Schechter, L. E., and Trimmer, J. S. (1996).  $\beta$ Subunits Promote K<sup>+</sup> Channel Surface Expression through Effects Early in Biosynthesis. *Neuron* 16 (4), 843–852. doi:10.1016/s0896-6273(00)80104-x
- Solé, L., Vallejo-Gracia, A., Roig, S. R., Serrano-Albarrás, A., Marruecos, L., Manils, J., et al. (2013). KCNE Gene Expression Is Dependent on the Proliferation and Mode of Activation of Leukocytes. *Channels* 7 (2), 85–96. doi:10.4161/chan.23258
- Vallejo-Gracia, A., Sastre, D., Colomer-Molera, M., Solé, L., Navarro-Pérez, M., Capera, J., et al. (2021). KCNE4-dependent Functional Consequences of Kv1.3-related Leukocyte Physiology. *Sci. Rep.* 11 (1), 14632. doi:10.1038/s41598-021-94015-9
- van Huizen, R., Czajkowsky, D. M., Shi, D., Shao, Z., and Li, M. (1999). Images of Oligomeric Kv $\beta$ 2, a Modulatory Subunit of Potassium Channels. *FEBS Lett.* 457 (1), 107–111. doi:10.1016/s0014-5793(99)01021-2
- Veatch, W. R., and Stryer, L. (1977). Effect of Cholesterol on the Rotational Mobility of Diphenylhexatriene in Liposomes: A Nanosecond Fluorescence Anisotropy Study. *J. Mol. Biol.* 117 (4), 1109–1113. doi:10.1016/s0022-2836(77)80017-x
- Vicente, R., Escalada, A., Soler, C., Grande, M., Celada, A., Tamkun, M. M., et al. (2005). Pattern of Kv $\beta$  Subunit Expression in Macrophages Depends upon Proliferation and the Mode of Activation. *J. Immunol.* 174 (8), 4736–4744. doi:10.4049/jimmunol.174.8.4736
- Vicente, R., Escalada, A., Villalonga, N., Texidó, L., Roura-Ferrer, M., Martín-Satué, M., et al. (2006). Association of Kv1.5 and Kv1.3 Contributes to the Major Voltage-dependent K<sup>+</sup> Channel in Macrophages. *J. Biol. Chem.* 281 (49), 37675–37685. doi:10.1074/jbc.M605617200
- Villalonga, N., Escalada, A., Vicente, R., Sánchez-Tilló, E., Celada, A., Solsona, C., et al. (2007). Kv1.3/Kv1.5 Heteromeric Channels Compromise Pharmacological Responses in Macrophages. *Biochem. Biophysical Res. Commun.* 352 (4), 913–918. doi:10.1016/j.bbrc.2006.11.120
- Wang, X., Zhang, J., Berkowski, S. M., Knowleg, H., Chandramouly, A. B., Downens, M., et al. (2004). Protein Kinase C-Mediated Phosphorylation of Kv 2 in Adult Rat Brain. *Neurochem. Res.* 29 (10), 1879–1886. doi:10.1023/b:nere.0000042215.92952.3d
- Włodarczyk, J., Woehler, A., Kobe, F., Ponimaskin, E., Zeug, A., and Neher, E. (2008). Analysis of FRET Signals in the Presence of Free Donors and Acceptors. *Biophysical J.* 94 (3), 986–1000. doi:10.1529/biophysj.107.111773
- Xu, J., and Li, M. (1997). Kv $\beta$ 2 Inhibits the Kv $\beta$ 1-Mediated Inactivation of K<sup>+</sup> Channels in Transfected Mammalian Cells. *J. Biol. Chem.* 272 (18), 11728–11735. doi:10.1074/jbc.272.18.11728
- Xu, J., Yu, W., Wright, J. M., Raab, R. W., and Li, M. (1998). Distinct Functional Stoichiometry of Potassium Channel  $\beta$  Subunits. *Proc. Natl. Acad. Sci. U.S.A.* 95 (4), 1846–1851. doi:10.1073/pnas.95.4.1846

**Conflict of Interest:** The authors declare that the research was conducted in the absence of any commercial or financial relationships that could be construed as a potential conflict of interest.

**Publisher's Note:** All claims expressed in this article are solely those of the authors and do not necessarily represent those of their affiliated organizations, or those of the publisher, the editors and the reviewers. Any product that may be evaluated in this article, or claim that may be made by its manufacturer, is not guaranteed or endorsed by the publisher.

Copyright © 2022 Roig, Cassinelli, Zeug, Ponimaskin and Felipe. This is an open-access article distributed under the terms of the Creative Commons Attribution License (CC BY). The use, distribution or reproduction in other forums is permitted, provided the original author(s) and the copyright owner(s) are credited and that the original publication in this journal is cited, in accordance with accepted academic practice. No use, distribution or reproduction is permitted which does not comply with these terms.